JMEPEG (2008) 17:621–626
DOI: 10.1007/s11665-007-9187-z

1059-9495/$19.00

Study of Flying Particles in Plasma Spraying

Fan Qunbo, Wang Fuchi, and Wang Lu

(Submitted March 5, 2007; in revised form November 7, 2007)

In this article, the trajectories of ceramic and metal particles in plasma spray are calculated by solving related momentum and energy equations. Meanwhile, the spatial distributions, temperatures, velocities, as well as diameters of the particles are measured by employing an online, in-flight particle sensor (DPV2000). The experimental and computational results are in good agreement. It has been found that the particle flying trajectories are dependent on material types and particle diameters, and in a plane vertical to the spraying axis, there is a certain corresponding relationship between the particle diameter and the particle velocity, as well as particle temperature.

Keywords particles trajectories, plasma spraying, spatial distribution

1. Introduction

In plasma spraying, particles are injected into the plasma jet, heated up, and accelerated. After that, they impact onto the substrate as molten droplets with high velocity, that cool and solidify to form coatings with excellent high-temperature resistance, wear resistance, or corrosion resistance.

During the plasma-spraying process, particles' velocity, temperature, as well as size significantly affect the final coating's microstructure and properties. On one hand, higher velocity helps to strengthen the interaction between the particles and the substrate, thus increasing the bond strength between the coating and the substrate; and higher temperature promotes the particles' melt fraction, thus increasing the effective contact area between the splat and the substrate, as well as the wetability, and bond strength. On the other hand, however, higher velocity means relatively shorter residence time of particles in the plasma jet, and particles cannot be heated enough to reach an ideal melting state, causing poor wettability, and difficulty in deposition, that lead to a coating with high porosity, low density, and poor mechanical strength. Higher temperature also means that the metal particles or the substrate are easily oxidized and yield poor bond strength, relatively larger residual stress, shorter service life, and poor reliability. Therefore, it is necessary to investigate the particles' trajectory, spatial distribution of particles' temperature, and spatial distribution of particles' velocity, as well as the relationships between these parameters and the particle diameter. For this reason, considerable attention has always been paid to research on flying particles in plasma spraying. In early days, for example, Vardelle and co-workers (Ref 1) investigated dynamic behavior of particles in the injector and plasma jet. In recent years, Xiong and Zheng (Ref 2) revealed the relationship between the particle melting status and the particle size, as well as the velocity. However, the interaction between the plasma jet and the particles, as well as the spatial distribution of particle groups of different materials still need further study.

Based on previous work on numerical simulation of multicomponent reacting plasma jet (Ref 3) and with respect to functionally gradient materials, particle traveling equations and the heat exchange model are incorporated into this research. Through calculating all of the equations and tracing the trajectory of the particles, the interaction between the plasma jet and the particles are simulated. In addition, by employing related experiments, the particle temperature, velocity and diameter of two different materials are measured, which are in good agreement with the calculation results. All the calculations in this article are performed by using a commercial computational fluid dynamics package, FLUENT (Ref 4).

Fan Qunbo, Wang Fuchi, and **Wang Lu**, Beijing Institute of Technology, Beijing 100081, China. Contact e-mail: fanqunbo@bit.edu.cn.

Nomenclature

a_1, a_2, and a_3	constants with different values of different *Re*
A_p	surface area of the particle
C_D	drag coefficient
c_p	specific heat of the particle
D_p	particle diameter
F_D	drag force per unit particle mass
H	convection heat transfer coefficient
I	electrical current
F_{Ar}	flow rate of argon
F_{He}	flow rate of helium
I_{in}	turbulent intensity
L_{in}	characteristic length
m_p	mass of the particle
Re	relative Reynolds number
T_a	the ambient temperature
T_p	particle temperature
T_∞	local gas temperature
v_p	particle velocity
v	gas velocity
ε_p	particle radiance
σ	the Boltzmann constant

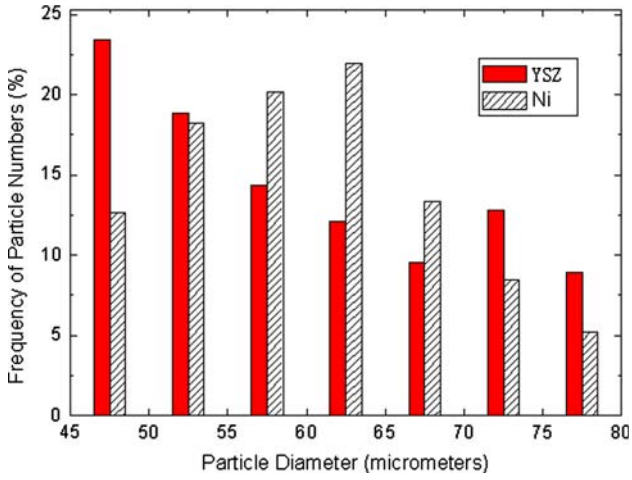

Fig. 1 Particle size distribution

Table 1 Basic physical properties of powders in plasma spraying (Ref 2)

	ρ_p, kg/m^3	c_p, J/kg K	k, J/s m K
YSZ	5560.0	456.1	1.85
Ni	8900.0	460.6	87.86

2. Experimental Details

2.1 Materials and Basic Properties

As raw materials of coatings, powders in plasma spraying largely determine the coating's physical and chemical properties. At the same time, materials themselves must meet the requirements of the plasma-spraying technology. In recent years, functionally gradient materials (FGM) of ceramic/metal systems have been commonly used, which have good properties of both ceramics and metals, e.g., excellent high-temperature resistance and corrosion resistance of ceramics, and good toughness of metals. Since yttria-stabilized zirconia (YSZ) and nickel (Ni) are two typical materials in FGM and widely used in the present time, this research is intended to do calculations and experiments related to these two materials, and investigate the particles' trajectories and diameter, velocity and temperature distribution in a plane vertical the spraying axis. Table 1 lists the basic physical properties of these two materials (Ref 5).

Figure 1 presents the particle size distribution, showing the frequencies (in percentage) of particle diameters for two different materials. It can be seen that, most YSZ particles are of small sizes within the range of 45-50 μm, and most Ni particles are of medium sizes within the range of 60-65 μm.

2.2 Processing Parameters

During the plasma-spraying process, a SG100 plasma gun (Praxair-TAFA) and a 1264 powder feeder (Sulzer Metco) are used, and the whole process is controlled by a computer. The feed rate of YSZ and Ni powders are kept constant at 23 g/min and 50 g/min, respectively. Table 2 lists the spraying parameters to different particles. For different materials, the operating parameters are also different.

Table 2 Thermal spraying parameters to different particles

	YSZ	Ni
Current (I)	500-900 A	500-900 A
Flow rate of Ar (F_{Ar})	50-90 scf/h	100-140 scf/h
Flow rate of He (F_{He})	0-40 scf/h	0-40 scf/h
Carrier gas flow rate	13 scf/h	15 scf/h

2.3 Measurements

In plasma spraying, the velocity, temperature, and diameter of the in-flight particles are measured using the online in-flight particle sensor for thermal spraying system, DPV-2000 (Tecnar Automation, Canada) (Ref 6). As illustrated in Fig. 2, the powder is fed from outside into the plasma gun. The sensor head of DPV-2000 measurement system is also vertical to the plasma jet. Measurements are carried out at X = 50, 60, 70, and 80 mm, respectively. At a fixed X position, 25 points in the plane YZ are set as measurement points, with a point-to-point interval of 3 mm. Prior to the measurement, the center of the plane is adjusted just around the center of the particle group, so as to observe as many flying particles as possible. It shall be noted that, whenever the operating parameters are changed, the plane at a fixed X position shall be moved, so as to get 25 new measurement points, since the deflection degree of the particles will be changed with the operating parameters, like current, gas flow rate, etc.

During the experiment, if the measurement values are not found to meet related requirements, the initial spray parameters are adjusted. For example, if most particles with relatively larger sizes do not melt, then the particle size is decreased accordingly. By analyzing the spatial distribution of particle temperature, velocity, and diameter, the effect of process parameters can be determined, thus deducing the final coating's quality.

3. Modeling Details

3.1 Theoretical Background

On the basis of the classical law of motion of particles in flowing fluid (Ref 7, 8), the velocity of a particle can be calculated according to the force balance on the particle:

$$\frac{d\vec{v_p}}{dt} = F_D\left|\vec{v} - \vec{v_p}\right|, \quad \text{(Eq 1)}$$

where $\vec{v_p}$ and $\vec{v}$ are the particle and gas velocities, respectively; F_D is the drag force per unit particle mass, which is given by

$$F_D = \frac{18\mu}{\rho_p D_p^2}\frac{C_D Re}{24}, \quad \text{(Eq 2)}$$

where, D_p is the particle diameter, C_D is the drag coefficient, and Re is the relative Reynolds number defined as

$$Re = \frac{\rho D_p\left|\vec{v} - \vec{v_p}\right|}{\mu} \quad \text{(Eq 3)}$$

The drag coefficient C_D is a function of the relative Reynolds number

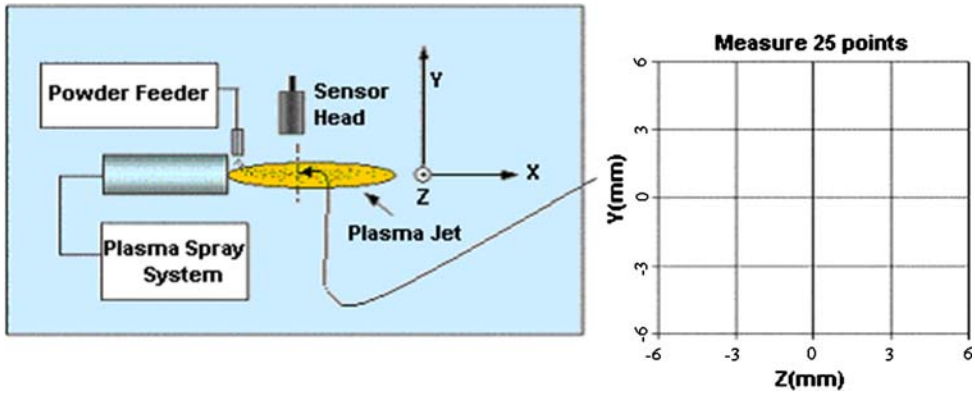

Fig. 2 Schematic of DPV-2000 diagnostic measurements

$$C_D = a_1 + \frac{a_2}{Re} + \frac{a_3}{Re^2} \quad \text{(Eq 4)}$$

where a_1, a_2, and a_3 are constants (Ref 8) with different values for different Re.

When the particle is in flight, heat will be transferred by convection and radiation between the particle and the plasma jet. Therefore,

$$m_p c_p \frac{dT_p}{dt} = hA_p(T_\infty - T_p) + \varepsilon_p A_p \sigma\left(T_a^4 - T_p^4\right) \quad \text{(Eq 5)}$$

where m_p is the mass of the particle, c_p is the specific heat of the particle, T_p is the particle temperature, T_∞ is the local gas temperature, h is convection heat transfer coefficient derived from the Nusselt number (Ref 9); ε_p is particle emissivity, A_p is the surface area of the particle, σ is the Boltzmann constant, and T_a is the ambient temperature. Equation 5 represents balance of the latent heat absorbed by particle (left side of the equation) and the heat interaction between the particle and the plasma jet (right side of the equation).

3.2 Geometric Model and Boundary Conditions

Figure 3 shows the geometry and computational domain. The computational domain is a 80 × 80 mm square. The outlet of the plasma gun is at the line AB, with a radius of 4 mm. The axial direction is set to x-coordinate, and the radial direction is set to y-coordinate. As can be seen in the figure, the outlet of the powder feeder is at the position, x = 8 mm, y = 13 mm. A rectangular mesh is used and subdivided in a non-uniform 80 × 80 grid. In the radial direction, the grid is more refined near the central axis and coarser toward the outer environment.

Boundary conditions, such as dynamic and thermodynamic conditions like turbulent intensity I_{in}, characteristic length L_{in}, temperature, pressure, as well as species mole fractions, at the locations AB, BC, CD, EF, FA, and DE can be specified according to the literature (Ref 10).

4. Results and Discussion

4.1 Flying Trajectories of Particles

Simulated particles' trajectories are shown in Fig. 4-6, with basic spray parameters: I = 800 A, F_{Ar} = 120 scf/h, and

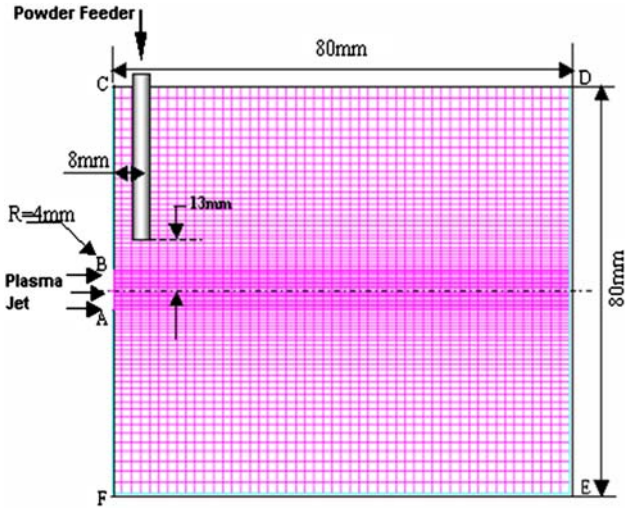

Fig. 3 Calculation domain

F_{He} = 10 scf/h. Figure 4 and 5 show the trajectories of YSZ and Ni particles with different diameters (particle diameter = 45-80 μm, particle number = 10), respectively. Figure 6 shows the flight trajectories of YSZ and Ni particles together (particle diameter = 45-80 μm, particle number = 20).

It can be seen that, flying particles' trajectories in plasma spraying are dependent on the particles' material type, as well as diameter. For particles of a certain material sprayed independently (see Fig. 4 and 5), particles with larger diameters penetrate more deeply into the plasma jet in the radial direction; for particles of different materials sprayed simultaneously (see Fig. 6), the particle groups will not overlap completely with each other. Since the density of Ni is higher than that of YSZ, Ni particle group will penetrate more deeply than YSZ in the radial direction.

Therefore, particle's density and diameter are the key factors that determine if the particle can penetrate into the plasma core or the high temperature zone and be heated sufficiently. Especially when spraying FGM, spray parameters shall be adjusted to ensure particle groups of different materials can overlap in a large degree. For example, Ni particles with larger density shall be selected as small-diameter ones. It might be noted, however, that the diameters must not be too small, so as to inhibit oxidation or evaporation.

4.2 Spatial Distribution of Particle Diameters, Velocities and Temperatures in a Fixed Plane

Figure 7-9 show the diameter, velocity, and spatial temperature distribution contour of YSZ and Ni particles in a *ZY* plane at x = 80 mm. All the data are measured at the predefined 25 points (see Fig. 2), and each value at each point is an arithmetic mean. In order to ensure that a sufficient number of particles are observed, operating parameters are different for different

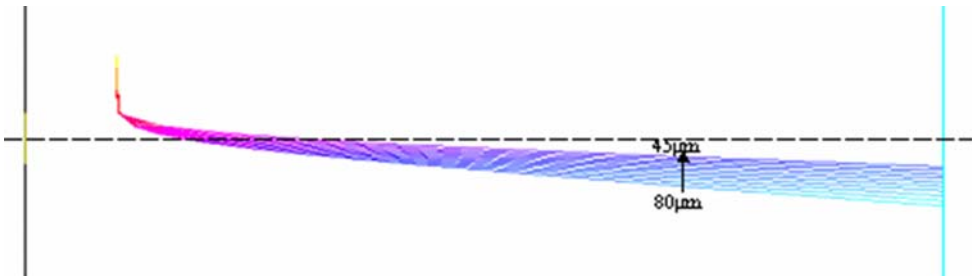

Fig. 4 Trajectories of YSZ particles with different diameters

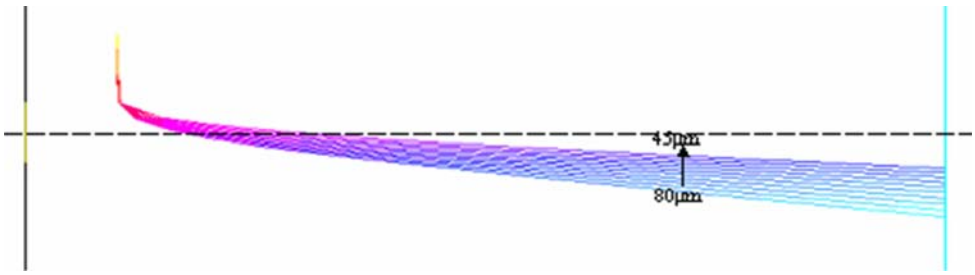

Fig. 5 Trajectories of Ni particles with different diameters

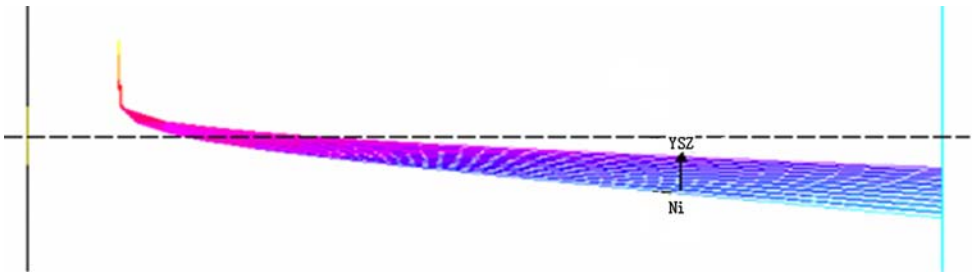

Fig. 6 Trajectories of co-sprayed particles

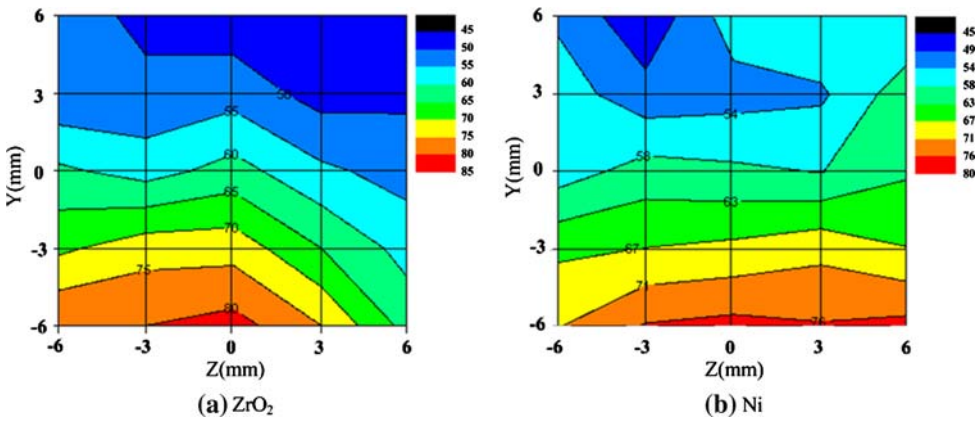

Fig. 7 Particle diameter spatial distribution contour (μm)

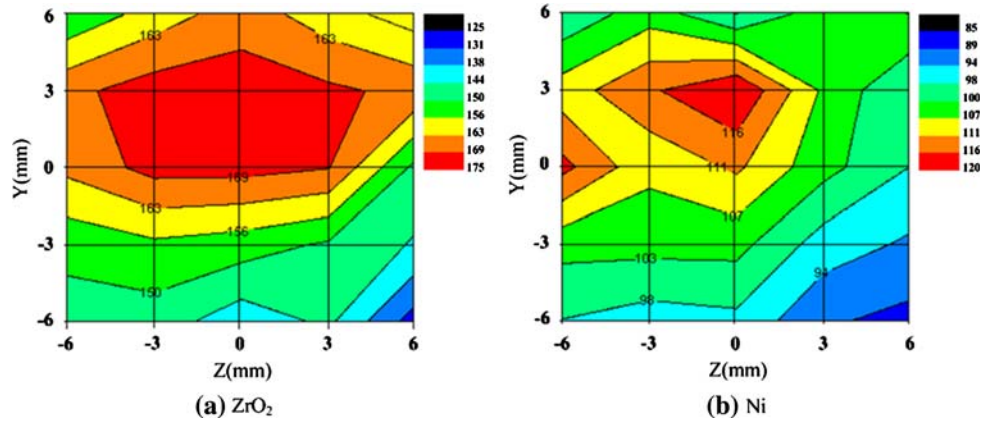

Fig. 8 Particle velocity spatial distribution contour (m/s)

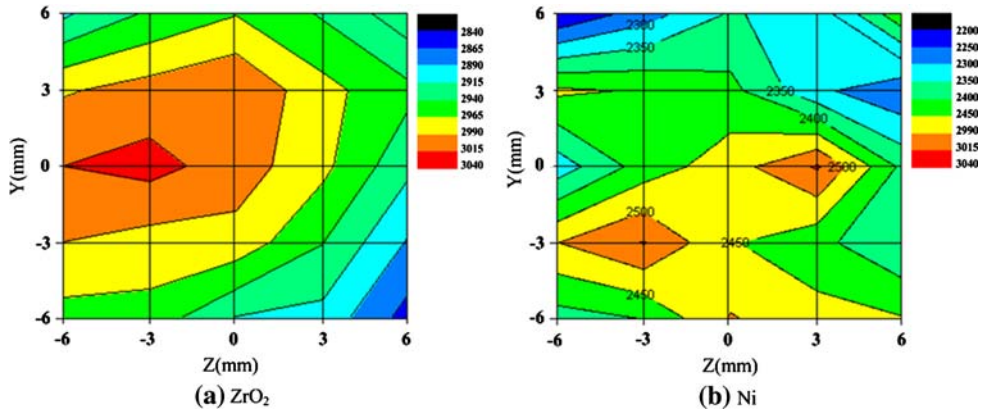

Fig. 9 Particle temperature spatial distribution contour (K)

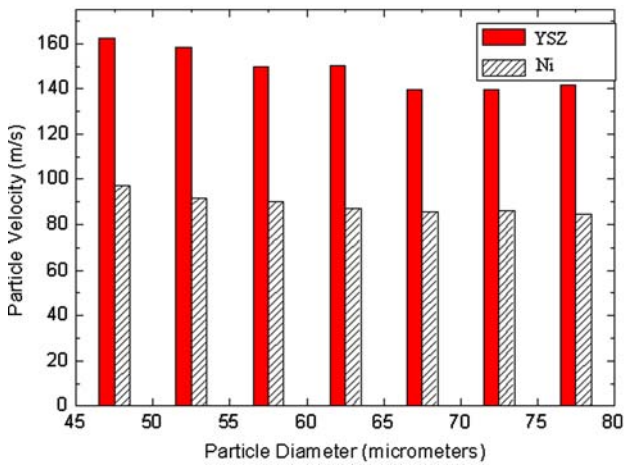

Fig. 10 Relationship between particle velocity and particle diameter (X = 80 mm)

materials. For ceramic material YSZ, I = 900 A, F_{Ar} = 70 scf/h, F_{He} = 30 scf/h; and for metal material Ni, I = 700 A, F_{Ar} = 120 scf/h, F_{He} = 30 scf/h.

As indicated in Fig. 7, when a particle group is entrained into the plasma jet in the direction of $-Y$ and reaches the position x = 80 mm (normally the substrate position), particles with different diameters arrive at different positions. For any material, particles of larger diameters always penetrate into the plasma jet more deeply than those with smaller diameters. Therefore, along negative Y-axis the particle diameter will increase, which is in good agreement with the simulated results in Fig. 4 and 5. Larger particles usually get relatively larger momentum under similar initial conditions, thus penetrating more easily into the plasma jet.

Figure 7 and 8 show that there is a specific correlation between particle velocity and particle diameter in the same ZY plane, that is, particles with larger diameter generally correspond to slower velocities. Usually, along negative Y-axis the particle velocity will decrease. Figure 10 presents the statistical averaged velocity histogram in a certain range of diameters. It can be seen that in a fixed plane vertical to the spraying axis, for either YSZ particle or Ni particle, particle velocity will decrease with increasing particle diameter. In Fig. 10, the velocities of Ni particles (86-97 m/s) are quite different from those of YSZ particles (140-162 m/s), which are determined by the spraying parameters and powder materials.

Particle temperature spatial distribution contour in the ZY plane shown in Fig. 9 indicates that particles with highest temperature are not located in the place where smallest particles are located, but nearly the center of the plasma jet (Y = 0). Figure 11 presents the statistical averaged temperature

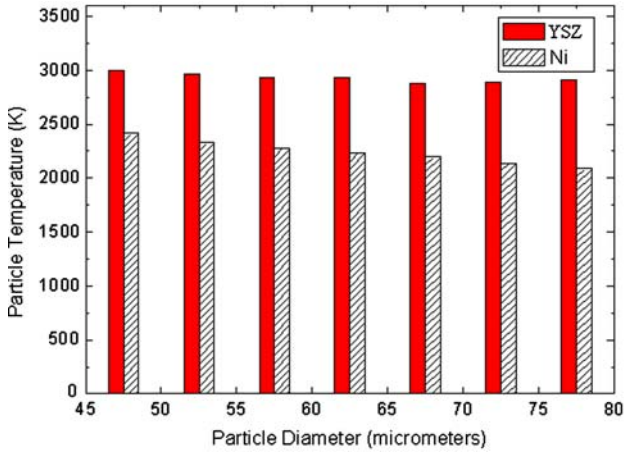

Fig. 11 Relationship between particle temperature and particle diameter (X = 80 mm)

histogram in a certain range of diameters. Although it illustrates a decrease of Ni particle temperature with increasing particle diameter, the YSZ particle temperature only changes slightly. Results in Fig. 9 and 11 show that particle temperature is determined not only by particle diameter, but also by whether it can be heated sufficiently. Larger particles may reside in the plasma jet long enough and reach relatively higher temperature; while smaller particles may be deflected from the plasma jet core and attain relatively lower temperature. This conclusion agrees well with the experimental results presented in the literatures (Ref 2, 11, 12).

5. Conclusions

In this article, with respect to two kinds of materials, velocity, temperature, and diameter of flying particles in plasma spraying are measured (by DPV-2000) and simulated. The numerical simulation method to indicate the interaction between the particle and the plasma jet is also presented. On the basis of calculated and measured results, the spatial distribution of particle velocity, temperature, and diameter is discussed and analyzed. The calculation results are in good agreement with the experimental results, which would be helpful to analyze the interaction between the particles and the substrate, as well as the formation of plasma sprayed coatings. The main conclusions are as follows:

(1) Particle-flight trajectories are determined by material types and particle diameters: for a certain material sprayed independently, particles with larger diameters penetrate more deeply into the plasma jet in the radial direction; while for particles of different materials sprayed simultaneously, particles with higher density penetrate more deeply than those with relatively lower density, and the particle groups will not overlap completely with each other.

(2) There is a specific relationship between the particle velocity and particle diameter, that is, larger particles usually have slower velocities; but there is not a similar relationship between the particle temperature and particle diameter, since particle temperature is affected not only by the diameter, but also by wheter the particle can be heated sufficiently in the plasma jet.

Acknowledgment

This support in part by the Commission of Science Technology and Industry for National Defense under Grant Number 9140A12020306BQ01 and the Excellent Young Teacher Foundation of Beijing Institute of Technology under Contract 1040012040101 was acknowledged.

References

1. M. Vardelle, A. Vardelle, B. Dussoubs, P. Fauchais, T.J. Roemer, R.A. Neiser, and M.F. Smith, Influence of Injector Geometry on Particle Trajectories: Analysis of Particle Dynamics in the Injector and Plasma Jet, in *Thermal Spray: Meeting the Challenges of the 21st Century*, C. Coddet, Ed., ASM International, Materials Park, OH, USA, 1998, p 887–894
2. H.-B. Xiong, L.-L. Zheng, L. Li, and A. Vaidya, Melting and Oxidation Behavior of In-flight Particles in Plasma Spray Process, *Int. J. Heat Mass Transfer*, 2005, **V48**, p 5121–5133
3. F. Qunbo, W. Lu, and W. Fuchi, 3D Simulation of the Plasma Jet in Thermal Plasma Spraying, *J. Mater. Process. Technol.*, 2005, **166**(2), p 224–229
4. *FLUENT 5.4 User's Guide*, Fluent Inc., Lebanon, 1998
5. R.H. Perry and D.W. Green, *Perry's Chemical Engineers' Handbook*. McGraw-Hill, USA, 1997
6. M. Krauss, D. Bergmann, U. Fritsching, and K. Bauckhage, In-situ Particle Temperature, Velocity and Size Measurements in the Spray Forming Process, *Mater. Sci. Eng. A*, 2002, **326**, p 154–164
7. L. Dayou, *Fluid Dynamics of Two Phases*. China High Education Press, Beijing, 1993
8. C. Kefa and F. Jianren, *Theory and Calculation of Industrial Gas and Solid Multi-phase Fluid*. Press of Zhe Jiang University, Hang Zhou, 1990 (in Chinese)
9. H.B. Xiong, L.L. Zheng, S. Sampath, R.L. Williamson, and J.R. Fincke, Three-dimensional Simulation of Plasma Spray: Effects of Carrier Gas Flow and Particle Injection on Plasma Jet and Entrained Particle Behavior, *Int. J. Heat Mass Transfer*, 2004, **47**(24), p 5189–5200
10. Y.Y. Zhao, P.S. Grant, and B. Cantor, Modelling and Experimental Analysis of Vacuum Plasma Spraying. Part I: Prediction of Initial Plasma Properties at Plasma Gun Exit, *Model. Simul. Mater. Sci. Eng.*, 2000, **8**, p 497–513
11. Z. Duan, L. Beall, and J. Schein, et al., Diagnostics and Modeling of an Argon/Helium Plasma Spray Process, *J. Therm. Spray Technol.*, 2000, **9**(2), p 225–234
12. M.P. Planche, R. Bolot, O. Landemarre, and C. Coddet, Comparison Between Experimental and Numerical Results Obtained on In-flight Particles Characteristics, in *Thermal Spray: Meeting the Challenges of the 21st Century*, C. Coddet, Ed., ASM International, Nice, France, 1998, p 355–360